

2

REPORT NO. NADC-89115-60

DTIC FILE COPY



HEAT AND MOMENTUM TRANSFER TO TEST SAMPLES IN THE HIGH VELOCITY PLASMA FURNACE

Stephen Russ and Thomas Kircher
Air Vehicle and Crew Systems Technology Department (Code 6063)
NAVAL AIR DEVELOPMENT CENTER
Warminster, PA 18974-5000

15 DECEMBER 1989

FINAL REPORT
Period Covering June 1989 to September 1989
Program Element No. 61153N

Approved for Public Release; Distribution is Unlimited

DTIC
ELECTE
MAY 31 1990
S E D

Prepared for
OFFICE OF NAVAL RESEARCH
Washington, DC 22217

NOTICES

REPORT NUMBERING SYSTEM — The numbering of technical project reports issued by the Naval Air Development Center is arranged for specific identification purposes. Each number consists of the Center acronym, the calendar year in which the number was assigned, the sequence number of the report within the specific calendar year, and the official 2-digit correspondence code of the Command Officer or the Functional Department responsible for the report. For example: Report No. NADC-88020-60 indicates the twentieth Center report for the year 1988 and prepared by the Air Vehicle and Crew Systems Technology Department. The numerical codes are as follows:

CODE	OFFICE OR DEPARTMENT
00	Commander, Naval Air Development Center
01	Technical Director, Naval Air Development Center
05	Computer Department
10	AntiSubmarine Warfare Systems Department
20	Tactical Air Systems Department
30	Warfare Systems Analysis Department
40	Communication Navigation Technology Department
50	Mission Avionics Technology Department
60	Air Vehicle & Crew Systems Technology Department
70	Systems & Software Technology Department
80	Engineering Support Group
90	Test & Evaluation Group

PRODUCT ENDORSEMENT — The discussion or instructions concerning commercial products herein do not constitute an endorsement by the Government nor do they convey or imply the license or right to use such products.

Reviewed By: J. Waldman Date: 2/2/90
Branch Head

Reviewed By: J. S. [Signature] Date: 3/26/90
Division Head

Reviewed By: W. J. Moroney Date: 3/24/90
Director/Deputy Director

UNCLASSIFIED

SECURITY CLASSIFICATION OF THIS PAGE

REPORT DOCUMENTATION PAGE				Form Approved OMB No. 0704-0188	
1a. REPORT SECURITY CLASSIFICATION Unclassified			1b. RESTRICTIVE MARKINGS		
2a. SECURITY CLASSIFICATION AUTHORITY			3. DISTRIBUTION / AVAILABILITY OF REPORT Approved for public release; distribution is unlimited		
2b. DECLASSIFICATION / DOWNGRADING SCHEDULE					
4. PERFORMING ORGANIZATION REPORT NUMBER(S) NADC-89115-60			5. MONITORING ORGANIZATION REPORT NUMBER(S)		
6a. NAME OF PERFORMING ORGANIZATION Air Vehicle and Crew Systems Technology Department		6b. OFFICE SYMBOL (If applicable) 6063	7a. NAME OF MONITORING ORGANIZATION		
6c. ADDRESS (City, State, and ZIP Code) Naval Air Development Center			7b. ADDRESS (City, State, and ZIP Code)		
8a. NAME OF FUNDING / SPONSORING ORGANIZATION Office of Naval Research		8b. OFFICE SYMBOL (If applicable)	9. PROCUREMENT INSTRUMENT IDENTIFICATION NUMBER		
8c. ADDRESS (City, State, and ZIP Code)			10. SOURCE OF FUNDING NUMBERS		
			PROGRAM ELEMENT NO. 61153N	PROJECT NO.	TASK NO.
			WORK UNIT ACCESSION NO.		
11. TITLE (Include Security Classification) (U) Heat and Momentum Transfer to Test Samples In the High Velocity Plasma Furnace					
12. PERSONAL AUTHOR(S) Stephen Russ and Thomas Kircher					
13a. TYPE OF REPORT Final		13b. TIME COVERED FROM 6/89 TO 9/89		14. DATE OF REPORT (Year, Month, Day) 1989 December 15	
15. PAGE COUNT 20					
16. SUPPLEMENTARY NOTATION					
17. COSATI CODES			18. SUBJECT TERMS (Continue on reverse if necessary and identify by block number)		
FIELD	GROUP	SUB-GROUP	Oxidation, High Temperature Coatings, Plasma, Heat Transfer		
19. ABSTRACT (Continue on reverse if necessary and identify by block number) A mass and heat transfer analysis was performed for two sample geometries under high temperature, high velocity air flow conditions. A qualitative picture of the flow fields expected during testing and the effects of the flow on heat transfer and skin friction are presented for square and cylindrical samples.					
20. DISTRIBUTION / AVAILABILITY OF ABSTRACT <input type="checkbox"/> UNCLASSIFIED / UNLIMITED <input type="checkbox"/> SAME AS RPT. <input type="checkbox"/> DTIC USERS			21. ABSTRACT SECURITY CLASSIFICATION		
22a. NAME OF RESPONSIBLE INDIVIDUAL Thomas Kircher			22b. TELEPHONE (Include Area Code) (215) 441-3804		22c. OFFICE SYMBOL 6063

DD Form 1473, JUN 86

Previous editions are obsolete.

SECURITY CLASSIFICATION OF THIS PAGE

S/N 0102-LF-014-6603

UNCLASSIFIED

UNCLASSIFIED

SECURITY CLASSIFICATION OF THIS PAGE

SECURITY CLASSIFICATION OF THIS PAGE

UNCLASSIFIED

CONTENTS

	Page
FIGURES	iv
NOMENCLATURE	v
BACKGROUND	1
OPERATING CONDITIONS	1
FACTORS AFFECTING HEAT AND MOMENTUM TRANSFER	4
HIGH-TEMPERATURE EFFECTS	4
VARIABLE PROPERTY EFFECTS	4
HIGH-SPEED EFFECTS	4
TURBULENCE EFFECTS	5
FLOW AROUND A CIRCULAR CYLINDER	5
TWO-DIMENSIONAL REGION	6
THREE-DIMENSIONAL REGION	6
CRITICAL REGIONS	10
FLOW AROUND A SQUARE CYLINDER	10
TWO-DIMENSIONAL REGION	10
THREE-DIMENSIONAL REGION	12
CRITICAL REGIONS	12
CONCLUSIONS	12
REFERENCES	14

FIGURES

Figure		Page
1	High Temperature Testing Facility	2
2	Sample in Test Section	3
3	2-D Region of Circular Cylinder in Crossflow	7
4	Circular Cylinder in Crossflow	8
5	3-D Flow Near Endwall	9
6	2-D Region of Square Cylinder in Crossflow	11
7	Square Cylinder in Crossflow	13

Accession For	
NTIS GRA&I	<input checked="" type="checkbox"/>
DTIC TAB	<input type="checkbox"/>
Unannounced	<input type="checkbox"/>
Justification	
By	
Distribution/	
Availability Codes	
Dist	Special
A-1	



NOMENCLATURE

ρ	Density
ν	Kinematic Viscosity
k	Thermal Conductivity
c_p	Gas Specific Heat
α	Thermal Diffusivity
T	Temperature
V	Gas Free Stream Velocity
D	Test Sample Diameter or Characteristic Dimension
r_c	Recovery Factor
h	Convective Heat Transfer Coefficient
τ_o	Wall Shear Stress (Skin Friction)
Pr	Prandtl Number (ν/α)
Re	Reynolds Number (VD/ ν)
Nu	Nusselt Number (hD/k)
C_f	Skin Friction Coefficient ($\tau_o/\rho V^2$)

THIS PAGE INENTIONALLY LEFT BLANK

BACKGROUND

The high-velocity plasma furnace is a unique facility that is currently under construction in the High Temperature Plasma Laboratory located in the Naval Air Development Center. The function of this facility will be to test materials under high-temperature, high-velocity air flow conditions.

In order to fully evaluate the results of exposure of a material to such a test it is useful to understand some of the important mass and heat transfer parameters involved. This report discusses the operating conditions of the testing facility and the factors which affect the heat, mass, and momentum transfer to the test samples. A qualitative picture of the flow fields expected during testing and effects of the flow on the heat transfer and skin friction will be presented. Two geometries, a circular cylinder and a square cylinder are considered. This report will provide information on where critical area of high heat transfer and skin friction exist.

OPERATING CONDITIONS

A schematic diagram of the high-velocity plasma furnace is shown in Figure 1. This testing facility is comprised of a nitrogen plasma torch which exits into the furnace test section. Samples are inserted via a ceramic mount into the test section.

The plasma torch is a high-mass flow rate nitrogen torch. It is designed to operate with a mass flow of 2200 SCFH nitrogen, a current of 470 amperes and a voltage drop of 400 volts. Oxygen is injected downstream of the anodes into the plenum to give the gas the approximate composition of air. This high-enthalpy gas then passes through a 4:1 contraction nozzle into the furnace test section. The furnace test section is a one-inch diameter, circular cross-section, insulated zirconia tube. The sample mount is located ten inches downstream from the furnace entrance. Two pyrometer ports are available for temperature sensing at this location.

The procedure for running a test on this facility involves first placing a sample into the ceramic mount and then inserting the sample into the furnace test section as shown in Figure 2. The plasma torch is then started and the furnace is slowly heated. This warm-up procedure takes about three hours.

At the design operating conditions, the temperature of the gas stream is about 3,400° F and the velocity is around 1,000 ft/s. These conditions yield a Reynolds number based on diameter of 17,500 for the flow through the test section. This is above the critical Reynolds number for turbulent pipe flow of 2,300. Sufficiently far downstream, one would therefore expect a fully developed turbulent velocity profile. The entry length for turbulent pipe flow is given as between 10 - 15 diameters but this depends on the entrance conditions¹. Since it is anticipated that the inlet flow will be very turbulent due to the upstream torch and mixing chamber, it is expected that the velocity profile will be nearly fully developed at the sample location (10 diameters downstream). The Prandtl number for the gas (air) at this temperature is 0.667. The furnace test section is well insulated. It is thus reasonable to expect the walls to be adiabatic and the temperature profile across the gas stream to be uniform. The sample mount is ceramic and insulates the test sample, very little heat will leave the test sample through the mount. During the test the sample will be fairly isothermal and approximately at the same temperature as the gas stream.

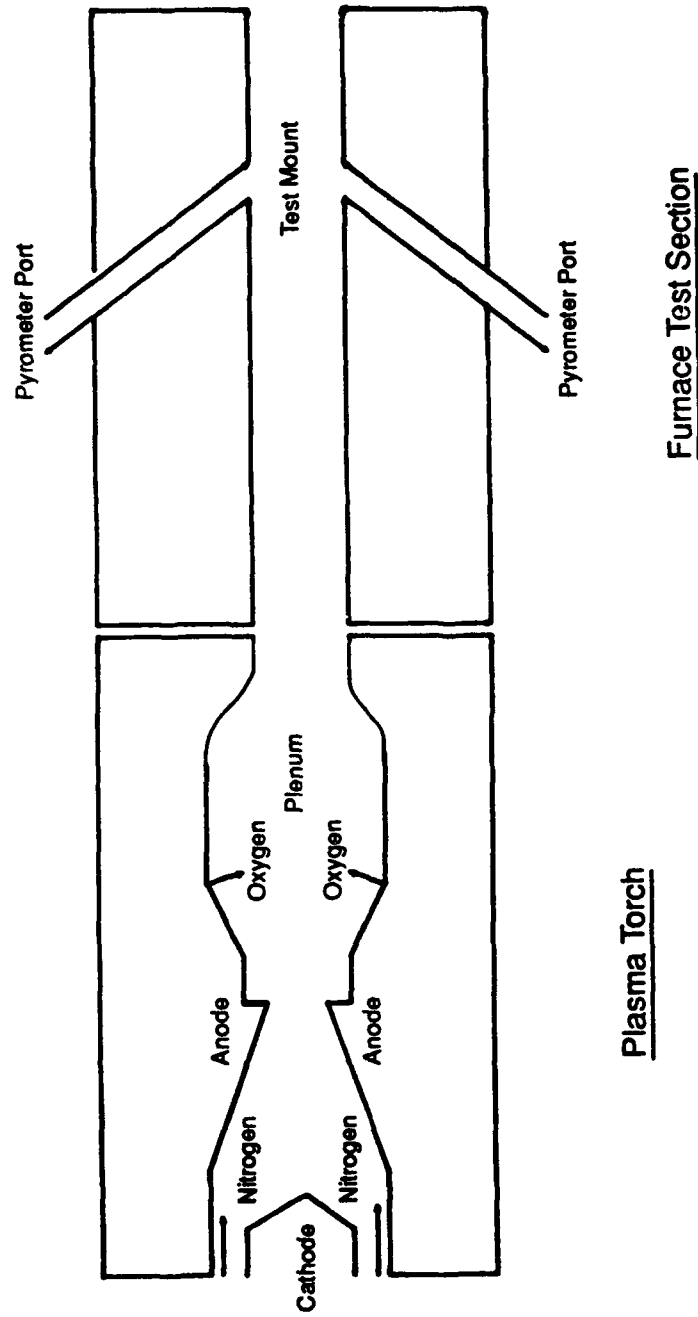


Figure 1. High Temperature Testing Facility.

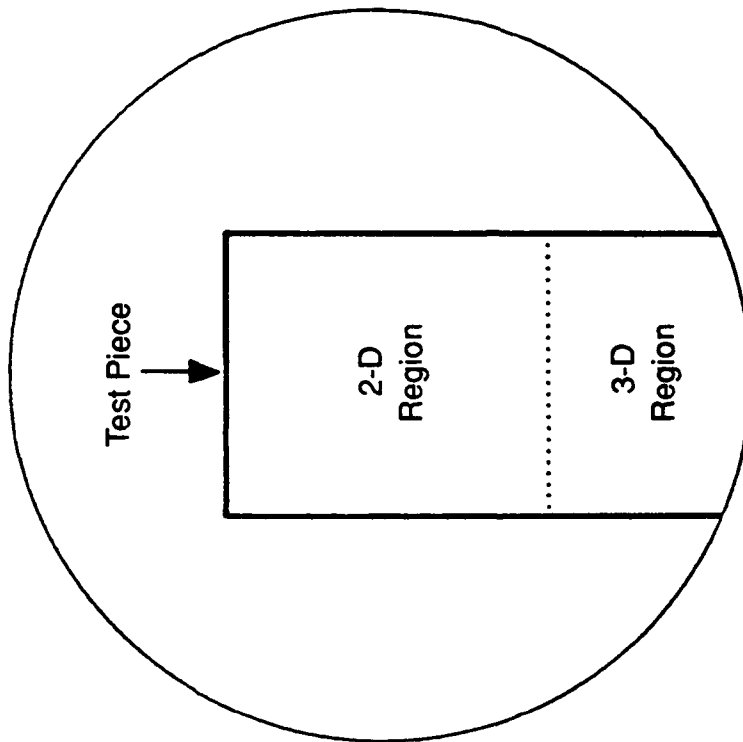


Figure 2. Sample in Test Section.

FACTORS AFFECTING HEAT AND MOMENTUM TRANSFER

HIGH-TEMPERATURE EFFECTS

The heat transfer from a very high temperature, partially dissociated or ionized gas can be very different than from a low temperature gas or liquid. The diffusion of these species through the boundary layer and their subsequent recombination results in different forms of energy transfer. The temperature of the gas at the sample location is about 3,400° F (2100° K). At this temperature these effects should not be significant. Oxygen and nitrogen dissociate at higher temperatures and become ionized at even higher temperatures.

VARIABLE PROPERTY EFFECTS

Most analytic convective heat transfer and skin friction solutions assume that fluid properties remain uniform throughout the flow field. The properties of gases and liquids vary significantly with temperature, however. This can result in a large variation in fluid properties across a boundary layer if the temperature difference is large. Two methods used to correct constant property solutions for variable property effects are in common use. These are the reference temperature method and the property ratio method ¹.

In the high-temperature testing facility the test samples are not actively cooled and the warm up period for the furnace is quite long (about three hours). It is therefore expected that the temperature of the test samples will be quite close to the temperature of the gas stream. The fluid properties can be evaluated at the gas stream temperature and the effect of slight property variations can be neglected.

HIGH-SPEED EFFECTS

High velocities result in different convective heat transfer due to the conversion of mechanical energy into thermal energy. This energy conversion may take place reversibly (as in a stagnation point flow) or irreversibly (as in a boundary-layer flow). Although these mechanisms are different, the method for correcting for the high speed effects are similar.

In a stagnation point flow, the temperature of the fluid outside the stagnation region boundary layer is the stagnation temperature. This is the fluid temperature resulting from an adiabatic deceleration and is defined as:

$$T^* = T + V^2/2c_p$$

The usual convective heat transfer solutions can be used by simply substituting the stagnation temperature for the free-stream temperature.

The boundary layer type of flow is more complicated but the correction method is similar. The usual heat transfer solutions are used by substituting the adiabatic wall temperature for the free-stream temperature. The adiabatic wall temperature is defined as:

$$T_{aw} = T + r_c V^2/2c_p$$

Where: $r_c = Pr$ for laminar boundary layers
 $r_c = Pr$ for turbulent boundary layers

In the high-temperature materials testing facility the design operating velocity is 1,000 ft/s and the temperature is 3,400° F. This results in a stagnation temperature of about 3,520° F. At this temperature the Prandtl number is 0.667 and thus the recovery factor (r_c) is 0.82 for laminar boundary layers and 0.87 for turbulent boundary layers. Thus the adiabatic wall temperature will differ from the stagnation temperature by only about 20°F for laminar boundary layers and 15° F for turbulent boundary layers. The use of the stagnation temperature for convective heat transfer calculations should be sufficiently accurate.

TURBULENCE EFFECTS

The level of disturbances in the free stream can have a large effect on fluid mechanics and convective heat transfer. A higher level of free-stream turbulence will cause a laminar boundary layer to undergo transition to a turbulent boundary layer sooner. This, in turn, will affect the boundary-layer development including the location of any separation points. Higher levels of free-stream turbulence also significantly increase convective heat transfer due to the higher turbulent transport.

The turbulence levels in the high-temperature materials testing facility are expected to be quite high due to the upstream plasma torch. The turbulence intensity in the center of the test section is expected to be between 3% and 4%. This is typical of the turbulence levels in fully developed turbulent pipe flows. This will cause about a 20% increase over low-turbulence convective heat transfer at stagnation points and in accelerating flow regions ².

The effect on heat transfer in non-accelerating regions and in separation zones will be small ³. The level of turbulence also has very little effect on the skin friction ³.

FLOW AROUND A CIRCULAR CYLINDER

The first sample geometry considered is a circular cylinder. At design conditions the free stream velocity ahead of the cylinder will be about 1,000 ft/s, the temperature will be 3,400° F and the test sample will have a diameter of 0.5 inches. This yields a Reynolds number based on diameter of 8,000. Small changes in the operating conditions will not have a large effect on the Reynolds number. This is well below the critical Reynolds number for turbulent boundary layers on a cylinder in crossflow ($Re = 150,000$) and therefore the boundary layers will remain laminar even though the free stream is very turbulent.

The flow around the cylinder will be considered in two parts. First the area of nominally two-dimensional flow is considered. This is the area where end effects are not important and starts about one diameter above the end wall (see Figure 2). Next, the three-dimensional region near the endwall is considered. In this area more complicated three-dimensional flow structures exist that have a strong influence on skin friction and heat transfer

TWO-DIMENSIONAL REGION

The flow around a cylinder in crossflow has been studied by numerous researchers. The flow in this case is slightly different because the fluid is constrained by the walls of the furnace test section. This results in a stronger acceleration around the cylinder and a slight delay in the separation of the laminar boundary layer. The basic regions of the flow should be similar to those found by other researchers, however. The predicted two-dimensional flow situation is shown in Figure 3.

At the leading edge of the cylinder a stagnation point region exists. A similarity solution exists for this type of two-dimensional stagnation point flow ¹. This solution shows that the skin friction increases linearly with distance from the stagnation point and the heat transfer coefficient is constant in this region.

After the stagnation point region the laminar boundary layer will experience a decreasing acceleration and therefore an increasing growth rate. The skin friction will continue to increase for a short distance due to the acceleration and then will begin to decrease as the boundary layer grows faster. The heat transfer coefficient will decrease in this region due to the growth of the thermal boundary layer.

Slightly before 90 degrees (see Figure 3) the flow will experience an adverse pressure gradient due to deceleration as the flow approaches the rear of the cylinder. This will cause the boundary layer to separate from the cylinder. At this point the skin friction goes to zero and the heat transfer coefficient assumes its minimum value.

After the separation point, a very turbulent wake exists at the rear of the cylinder. The skin friction will be very small in this recirculating flow region. The heat transfer coefficient will increase in this region due to the high mixing caused by the separation and vortex formation ⁴.

Figure 4 shows the expected skin friction and heat transfer coefficient distributions in the two-dimensional region. These are presented in non-dimensional form and are valid only in a small range of Reynolds numbers in the neighborhood of the expected operating conditions ($Re = 5,000 - 10,000$). The heat transfer coefficient near the stagnation point was calculated from the stagnation point similarity solution ¹.

This value was increased 20% due to the expected high-turbulence intensity ². The angular variation in the heat transfer coefficient was assumed to be similar to the experimental results of Reference 5. The overall average heat transfer coefficient was taken to be similar to experimental correlations ⁴. The skin friction in the stagnation point region was taken from the similarity solution ¹. The angular distribution of the skin friction was predicted from a similarity solution ².

THREE-DIMENSIONAL REGION

The flow at the base of the cylinder is more complicated due to the interaction of the endwall boundary layer with the cylinder. The vorticity in the endwall boundary layer causes a large horseshoe vortex to roll-up at the base of the cylinder. An excellent flow visualization of this vortex is given in Reference 6. There also exists evidence of a smaller counter-rotating corner vortex between the horseshoe vortex and the base of the cylinder under certain conditions ⁷. A schematic diagram of these vortices is shown in Figure 5. These vortices are convected around the cylinder and therefore affect the flow on the sides of the cylinder as well as the flow at the leading edge stagnation point region.

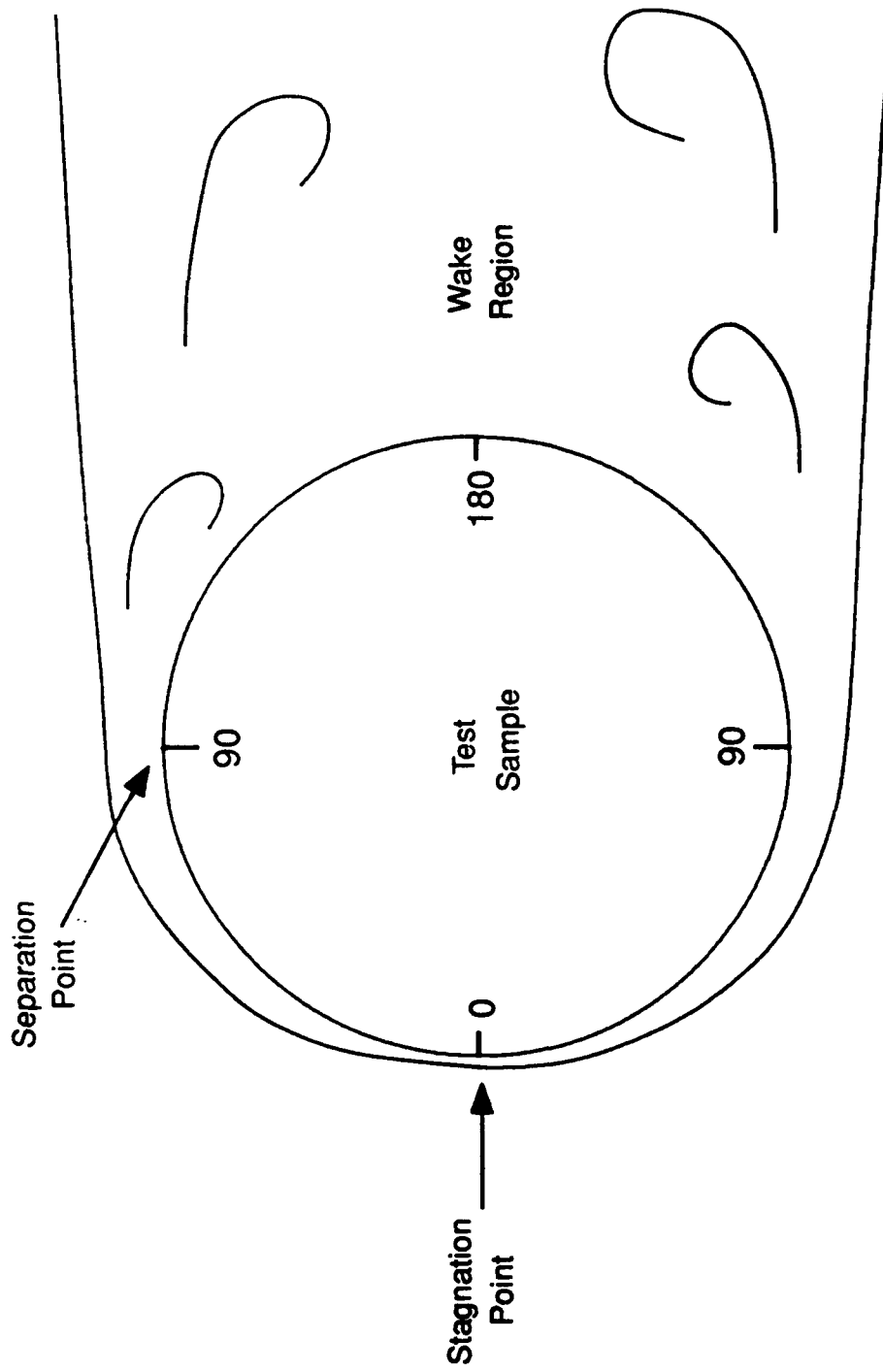


Figure 3. 2-D Region of Circular Cylinder in Crossflow.

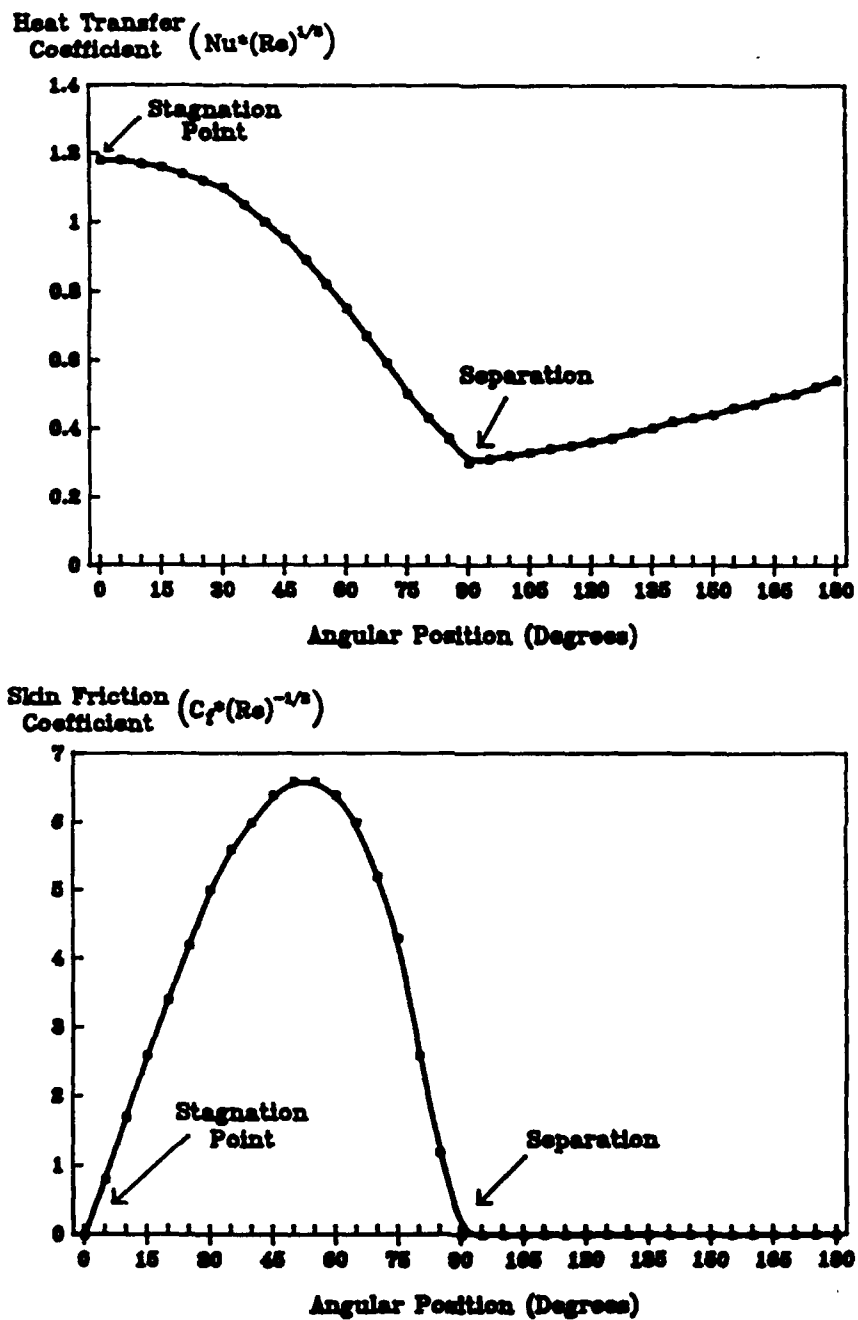


Figure 4. Circular Cylinder in Crossflow.

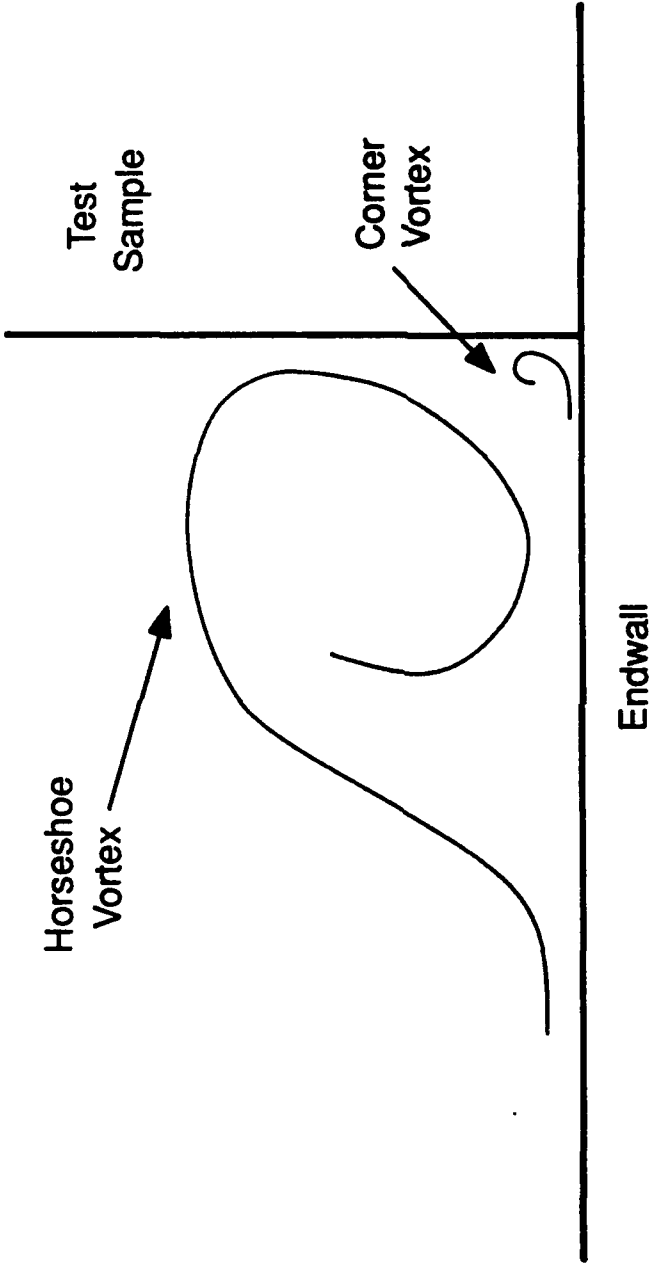


Figure 5. 3-D Flow Near Endwall.

An exact prediction of the formation of these vortices and their effect on heat and momentum transfer is difficult. The formation of the vortices is dependent upon geometry. The curvature of the endwall (see Figure 2) and the geometry of the sample mount make this geometry slightly different than that of other researchers. An estimate of the enhancement in heat transfer and skin friction can be found from the mass transfer results of Reference 7. Based on these results an increase in local heat transfer and skin friction of up to 50% is possible due to the horseshoe vortex and even higher augmentation is possible if a corner vortex is formed.

CRITICAL REGIONS

The region of highest heat transfer will occur at the base of the cylinder in the stagnation point region. Here the vortices will greatly enhance the already high stagnation-point heat transfer. The region of highest skin friction will occur at the base of the cylinder at an angular position near 50 degrees (Figure 3). This is because of the strong acceleration and three-dimensional flow structures that exist in this region. A critical region may also exist at the top of the test sample if the edges are sharp. The edges will cause a strong acceleration and therefore high heat and momentum transfer.

FLOW AROUND A SQUARE CYLINDER

The test conditions for this sample will be similar to the circular cylinder test conditions. The gas velocity will be about 1,000 ft/s, the gas temperature will be 3,400° F and the sample size will be 0.5 inches on a side. This yields a Reynolds number of 8,000 based on side length.

The flow around this sample geometry is considered in a similar manner as the flow around a circular cylinder. First the 2-D region is discussed and then the more complicated 3-D region at the base of the square cylinder is considered.

TWO-DIMENSIONAL REGION

This geometry has not been as extensively studied as the circular cylinder, however, the basic flow regimes are still well understood. The expected flow situation is diagrammed in Figure 6.

The leading face of the square cylinder will be a stagnation point region. The flow stagnates at the center of this face and accelerates along the face. A similarity solution exists for this type of stagnation point flow. This solution shows that the shape of the velocity profile and the boundary layer thickness remain constant ². The skin friction increases linearly from the stagnation point and the heat transfer coefficient remains essentially constant. The acceleration will become stronger near the edges of the front face. This will result in increased skin friction and heat transfer.

At the corners of the front face the boundary layers will separate from the sample resulting in a recirculation zone on the side faces of the sample. At this moderate Reynolds number the flow will probably reattach to the side faces of the cylinder. This reattachment was observed at a Reynolds number of 18,000 in a mass transfer study ⁸. This reattachment results in a large increase in skin friction and heat transfer. The exact location of the reattachment point cannot be predicted due to a lack of other experimental data.

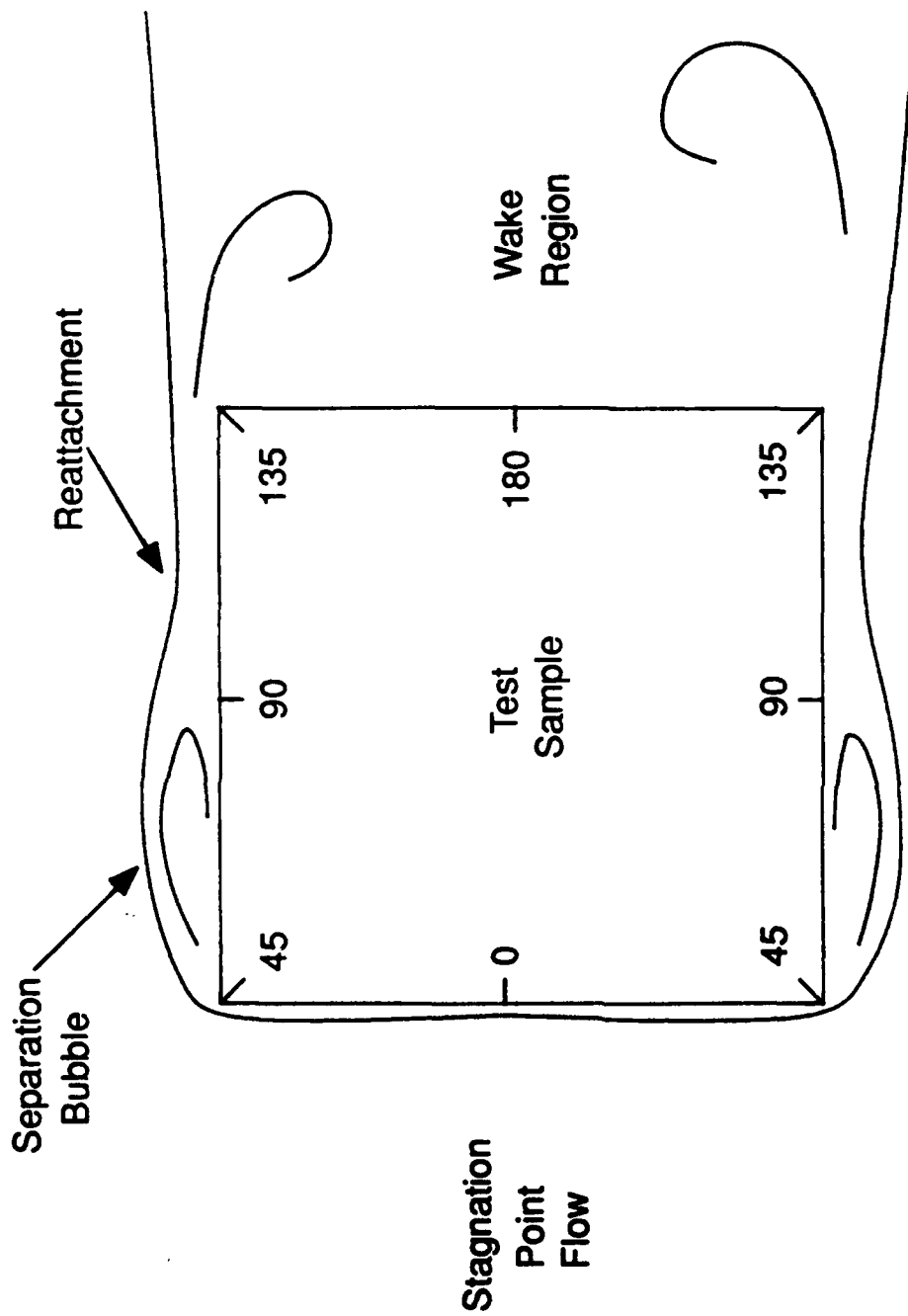


Figure 6. 2-D Region of Square Cylinder in Crossflow.

The flow will again separate at the downstream edge of side faces resulting in a large wake region at the rear of the sample. The downstream face will experience moderate heat transfer due to the strong mixing in this region. The skin friction will be very small in this recirculation zone.

The predicted heat transfer coefficient and skin friction distributions for this sample in the 2-D region are shown in Figure 7. The overall average heat transfer coefficient was predicted from an experimental correlation ⁴. The stagnation point heat transfer was predicted from the average heat transfer coefficient and the similarity solution. The local variations in the heat transfer coefficient were predicted from the analogous mass transfer results of Reference 8. The skin friction on the front face was predicted from the stagnation point similarity solution and the assumed velocity distribution. The skin friction prediction in the reattachment region is only an estimate. The exact reattachment location and the characteristics of the reattached boundary layer cannot be accurately predicted.

THREE-DIMENSIONAL REGION

The vorticity in the approaching boundary layer will cause the formation of a horseshoe vortex at the base of the test sample. A smaller but stronger corner vortex may also be formed ⁸. A diagram of these vortices is shown in Figure 5. An exact prediction of these flow structures is difficult because their formation is dependent upon geometry. The curvature of the endwall (Figure 2) and the geometry of the sample mount make this geometry slightly different than that of other researchers.

The result of these vortices will be enhanced heat and momentum transfer in the endwall region. An accurate quantitative prediction in this case is impossible because of the large uncertainties in the flow structures and a lack of other experimental data. Based on mass transfer studies ⁸ an enhancement of up to 50% in local heat transfer and skin friction is possible due to the horseshoe vortex and even higher enhancements are possible due to the corner vortex, if it is formed.

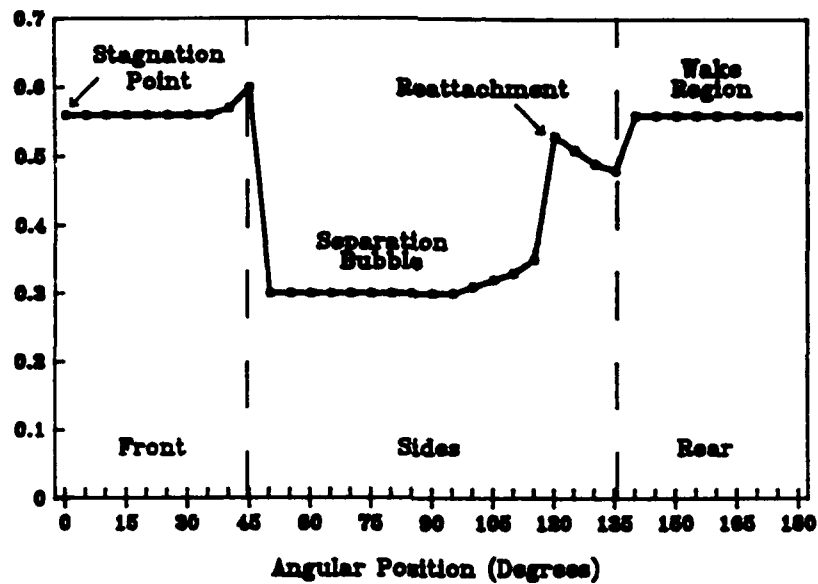
CRITICAL REGIONS

The area of highest heat transfer will be on the corners of the leading face, near the endwall. The curvature of the test section (Figure 2) causes the highest acceleration near the endwall. The flow structures formed at the endwall and this strong acceleration around the cylinder will result in the highest heat transfer. The area highest skin friction will also be at the corners of the front face near the endwall for the same reasons.

CONCLUSIONS

This paper has made analytical predictions of the heat transfer and skin friction distributions for test samples in the high-velocity plasma furnace facility. The critical regions for any sample inserted into this furnace will be near the endwall and at any sharp edges. The formation of three-dimensional flow structures in the endwall region will result in large augmentation of the heat and momentum transfer. The strong acceleration caused by flow around any sharp edges will also result in high heat transfer and skin friction.

Heat Transfer Coefficient ($Nu \cdot (Re)^{-1/2}$)



Skin Friction Coefficient ($C_f \cdot (Re)^{-1/2}$)

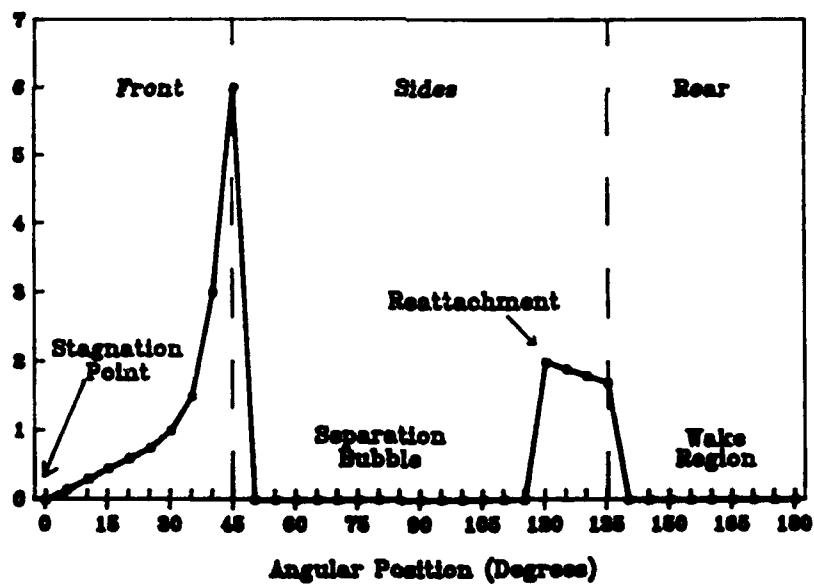


Figure 7. Square Cylinder in Crossflow.

REFERENCES

1. Kays, W.M. and Crawford, M.E., 1980, Convective Heat and Mass Transfer, McGraw-Hill
2. Schlichting, H., 1979, Boundary Layer Theory, McGraw-Hill
3. Kestin, J., 1966, "The Effect of Free-Stream Turbulence on Heat Transfer Rates", Advances in Heat Transfer, Vol. 3, Academic Press
4. Incropera, F.P. and DeWitt, D.P., 1985, Introduction to Heat Transfer, John Wiley and Sons
5. Giedt, W.H., 1949, "Investigation of variation of point unit heat transfer coefficient around a cylinder normal to an airstream.", Trans. of ASME, Vol. 71, p. 375-381
6. Van Dyke, M., 1982, An Album of Fluid Motion, The Parabolic Press, p. 55
7. Goldstein, R.J. and Karni, J., 1984, "The Effect of a Wall Boundary Layer on Local Mass Transfer from a Cylinder in Crossflow", ASME Journal of Heat Transfer, Vol. 106, No. 2
8. Goldstein, R.J., Yoo, S.Y. and Chung, M.K., 1989, "Mass Transfer from a Square Cylinder and its Endwall in Crossflow", to appear in Int. J. of Heat and Mass Transfer

Distribution List
Report No. NADC-89115-60

	No. of Copies
Los Alamos National Laboratory	1
Los Alamos, NM 87543	
(1 Copy for J. Petrovic)	
NIST	1
Washington, DC 20234	
(1 Copy for E. Fuller)	
NASA	1
George C. Marshall Space Flight Center	
Marshall Flight Center, AZ 35812	
(1 Copy for B. Goldberg)	
Wright Patterson AFB, OH 45433	1
(1 Copy for R. Kerans) AFWAL/MLLM	
Naval Air Development Center	5
Warminster, PA 18974-5000	
(2 Copies for Code 8131)	
(3 Copies for Code 6063; T. Kircher)	

Distribution List
Report No. NADC-89115-60

	No. of Copies
Naval Air Propulsion Center	1
P.O. Box 7176	
Trenton, NJ 08628-0176	
(1 Copy for R. Mahorter)	
 Naval Research Laboratory	 1
Washington, DC 20375	
(1 Copy for 6360; D. Lewis)	
 Naval Surface Weapons Center	 3
Dalgren, VA 22448-5000	
(1 Copy for C. Rowe)	
(1 Copy for M. Opeka)	
(1 Copy for R. Edwards)	
 Office of Naval Research	 1
800 North Quincy Street	
Arlington, VA 22217-5000	
 NASA Langley Research Center	 1
Hampton, VA 23665	
(1 Copy for Code 188M; Robert Swann)	
 Office of Naval Technology	 1
Washington, DC 22217	
(1 Copy for J. Kelly)	
 Naval Air Systems Command	 1
Washington, DC 20361-0001	
(1 Copy for AIR-931-A; L. Slotter)	
 Defense Technical Information Center	 2
ATTN. DTIC-FDAB	
Cameron Station BG5	
Alexandria, VA 22304-6145	
 Center for Naval Analysis	 1
4401 Fort Avenue	
P.O. Box 16268	
Alexandria, VA 22302-0268	
 Defense Advanced Research Projects Agency	 1
Washington, DC 22209	
(1 Copy for Code DSO/MSD; W. Barker)	